Prasanna, Malith; Polojärvi, Arttu; Wei, Mingdong; Åström, Jan A.

Bonded particle simulation of fragmenting ice blocks

Published in:
Proceedings of the 26th IAHR International Symposium on Ice

Published: 01/01/2022

Document Version
Publisher's PDF, also known as Version of record

Please cite the original version:
Prasanna, M., Polojärvi, A., Wei, M., & Åström, J. A. (2022). Bonded particle simulation of fragmenting ice blocks. In *Proceedings of the 26th IAHR International Symposium on Ice* (IAHR International Symposium on Ice). International Association for Hydro-Environment Engineering and Research.

IAHR AIRH

26th IAHR International Symposium on Ice
Montréal, Canada – 19-23 June 2022

Bonded Particle Simulation of Fragmenting Ice Blocks

Malith Prasanna[1], Arttu Polojärvi[1], Mingdong Wei[1], Jan Åström[2]
[1]Aalto University School of Engineering,
Department of Mechanical Engineering, P.O. Box 14100, FI-00076 Aalto, Finland
[2]CSC-IT-Center for Science,
P.O. Box 405, FI-02101 Espoo, Finland
malith.prasanna@aalto.fi

This paper describes bonded particle method-based modeling of ice blocks failing under compressive ice-to-ice contacts. Ice block contacts transmit ice loads; thus, local failure of ice blocks has an important role in ice-structure interaction processes. The model is shortly described and laboratory-scale experiments on saline ice block failure are modeled. Simulations yield results, which compare well with the experiments in terms of failure patterns and the force transmitted by the contacts. The local failure of the ice blocks at the contacts occurs predominately by a shear-like failure governed by the bulk strength of the material with characteristics of Coulombic shear faults. The results imply that the traditional crushing dominated failure models for local failure at the contacts of ice blocks in numerical simulations might not be valid. Instead, shear failure of ice should be accounted.

1. Introduction

Crushing and fragmentation of ice under compression have a key role in ice-structure interaction processes. An ice block subjected to compression could fail through various failure modes such as splitting, shearing, spalling and crushing. The failure mode depends on the loading rate, direction of the forces relative to the grain direction and confinement of the ice specimen (Schulson and Nickolayev, 1995; Schulson and Gratz, 1999). Moreover, friction, local confinement, and local deformation may also influence the failure mode (Schulson *et al*., 1989, Kuehn *et al*., 1993). Thus, numerical modeling of compressive failure of ice can be a demanding exercise. Here we use a Bonded Particle Method (BPM) model to numerically reproduce the laboratory experiments on saline ice blocks broken under compressive ice-to-ice contacts (Prasanna *et al*., 2021).

In the experiments modeled here, three 300 mm × 300 mm × 110 mm naturally grown saline ice blocks were set to form two ice-to-ice contacts as presented in the Figure 1(a) and compressed until the failure of the three-block system. The ice tested was rather warm with the mean temperature of -2.5 ºC as the blocks were floating in saline water. The compressive force, F_p, force transmitted by each contact, F_1 and F_2, and failure process were recorded. The experiments were conducted for six contact lengths, c =25,50,75,100,125 and 150 mm. The ice blocks failed predominantly by a shear-band formation as shown in the Figure 1(b). The failure, thus, was related to the bulk strength of the material.

We simulated the ice block breakage experiments by using the BPM tool HiDEM (Helsinki Discrete Element Model) (Åström *et al*., 2013; Todd *et al*., 2018). Two-fold objectives of our simulations are (1) to study the numerical techniques that can be used to simulate the quasi-brittle compressive failure of ice and (2) to investigate the detailed mechanics of the failure process itself. The study increases understanding of compressive failure of ice in engineering scale applications, such as local failure at contacts of a pair of blocks in a force chain, as well as geophysical scale phenomena such as edge failure of two colliding ice floes. The paper summarizes the findings presented in Prasanna *et al*. (2021, 2022).

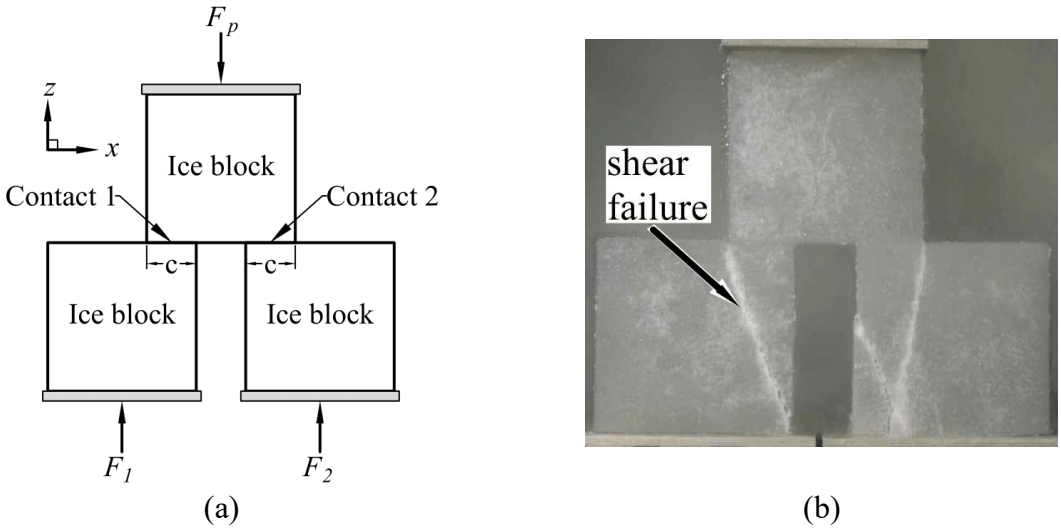

Figure 1. (a) Illustration of the three-blocks system and (b) shear failure of the ice blocks. Each ice block was of size 300 mm × 300 mm × 110 mm. Figure reproduced from Prasanna *et al*. (2022).

2. Modeling of ice in HiDEM

HiDEM model and the requirements for modeling columnar grained ice by using HiDEM is described in detail in Prasanna *et al*. (2022). In brief, ice is modeled as a lattice of dense packed spherical particles connected by Euler-Bernoulli beam elements. A beam can break by a cohesive crack forming at one of its ends, which mimics the formation of micro-cracks. The cohesive crack dissipates the elastic energy stored in the beam and gradually brings down the internal forces to zero, which replicates material softening during quasi-brittle failure. The cohesive softening model implemented in HiDEM is based on the work by Paavilainen *et al.* (2009). Coalescence of the micro cracks eventually leads to the ultimate failure of beam-sphere lattice. Contact interaction between spheres is modeled by using a Hertzian contact model, where the contact force is proportional to the overlap between spheres. Energy dissipation is modeled by using a viscous damping model.

The beam lattice topologies in BPM models have significant bias on the failure paths (Jirásek and Bažant, 1995). Thus, a beam-sphere lattice replicating the grain structure of naturally grown columnar ice, termed anisotropic micro-structure model (AMSM), was used in this work. Naturally grown ice has a vertically aligned columnar grained micro-structure, with the grains aligned parallel to the direction of ice growth. Therefore, the AMSM was created so that the particles in lattice are randomly placed in the horizontal plane with hexagonal closed packing in the vertical plane. Figures 2(a) and (b) show the horizontal and vertical cross sections of the AMSM respectively. When modeling the three-block failure experiments (Figure 1), the simulations contained about 6×10^5 particles with radii distribution of 70% 2 mm and 30% 1.5 mm.

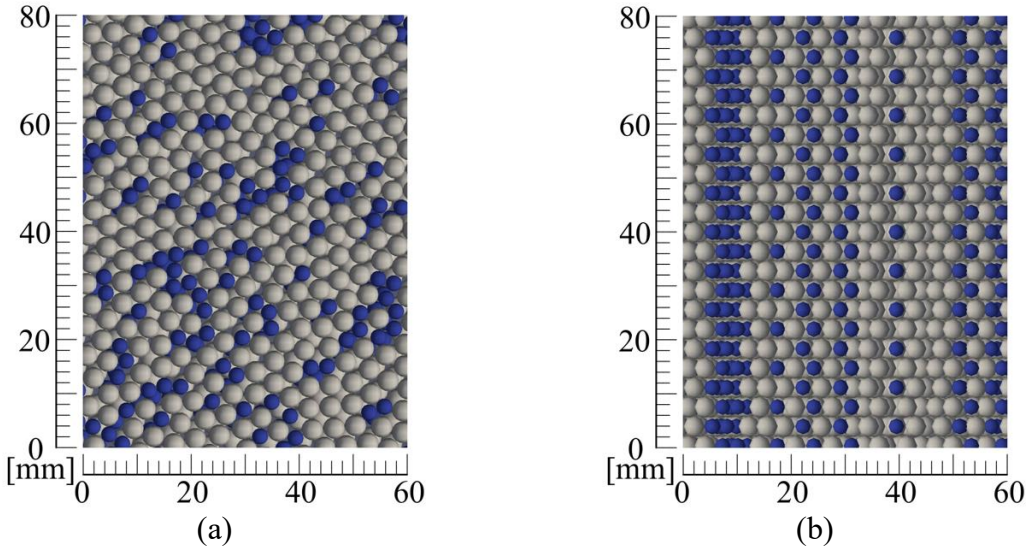

Figure 2. (a) Horizontal and (b) Vertical cross sections of ice modeled by HiDEM. The figures illustrate the anisotropic micro-structure model (AMSM). Here, blue and grey particles have 1.5 mm and 2 mm radius respectively. Figure reproduced from Prasanna *et al*. (2022).

3. Results

Three-block breakage experiments were simulated using the HiDEM for all the contact lengths tested in the experiments. Each *c* was simulated using six different sphere packings to account for the potential scatter in simulation results. Figure 3 presents typical failure patterns and force-time (*F*-*t*) curves from the simulations for *c* =50,100 and 150 mm respectively.

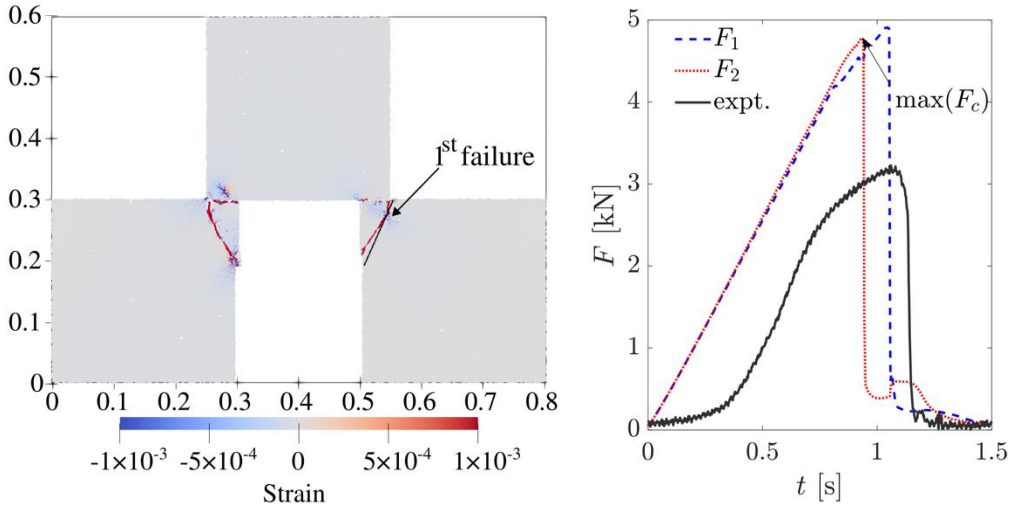

(a)

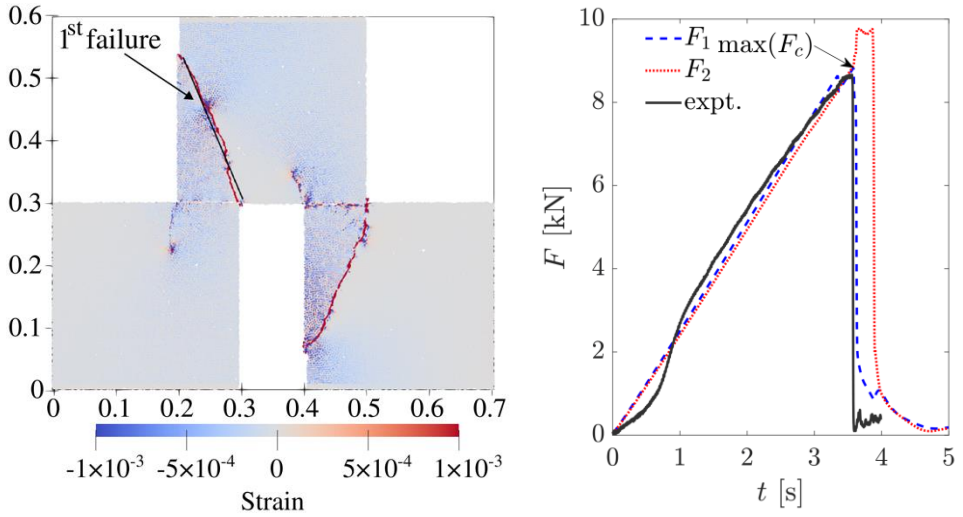

(b)

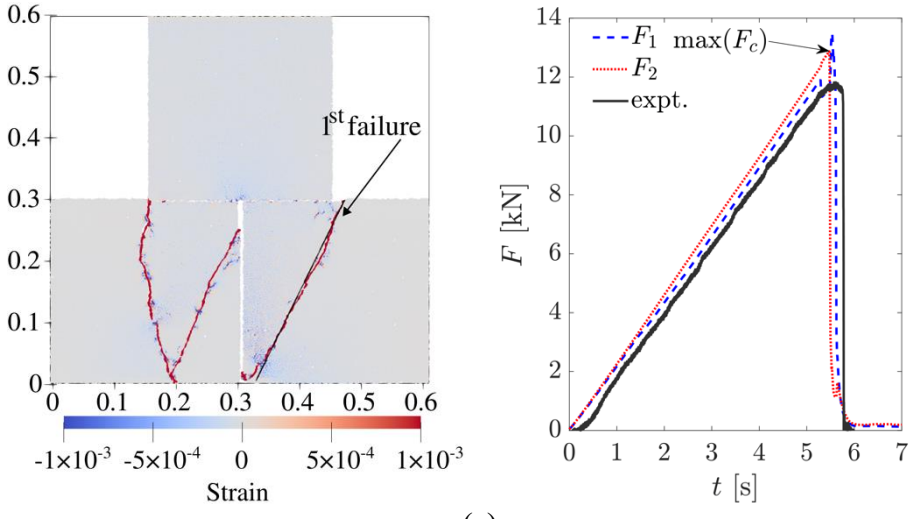

(c)

Figure 3. Failure patterns and *F*-*t* curves of three block breakage experiment simulations: (a) contact length c =50 mm, (b) c =100 mm and (c) c =150 mm. The black line in failure pattern figures are failure planes predicted by using the Mohr-Coulomb failure criterion. Figure reproduced from Prasanna *et al*. (2022).

As shown in the figures, the first failure of the ice blocks was predominantly due to shear faulting. This agrees well with the experiments, where about 75 % of the specimens failed due to shear. The analysis focused on the first contact to fail only, since the loading conditions for the second contact changed after the first failure. The failure of the second contact, showed a mixed behavior including shear faults and running shear cracks plausibly due to the increase of the contact force after the first failure.

Figure 3 further compares the *F-t* curves from the simulations with the experimental ones. The simulated *F-t* curves follow the general trend of the experimental curves, excluding the case with c =50 mm. The maximum contact force transmitted by the first contact to fail, max(F_c), increased with the contact length. Failure force of the second contact to fail was about 20% higher than max(F_c). Non-linear initial part of the experimental *F-t* curves, significant in the c =50 mm experiments, was due to initial misalignment of the blocks and ice blocks settling at the contacts. Simulations do not capture this behavior, thus, the simulated *F-t* curves for cases c =50 mm deviate from the experimental data. As c increases, the significance of the local deformations at the contact gradually decreases. For the cases c >50 mm, the simulations captured the *F-t* curve of the three-block system well.

For the shear-like failure, critical shear force, F_τ, and critical normal force, F_n, acting on the shear plane [as presented in Figure 4(a)] was calculated by resolving the max(F_c) in respective directions. Further, the area of the shear plane, A_τ, was calculated by multiplying the shear plane length by the thickness of the ice block. Figure 4(b) shows F_τ plotted against A_τ in the simulations and the experiments. The figure also shows trend lines fitted to the simulation and experimental data. The simulated and experimental results agree well. Furthermore, the data points corresponding to different c are overlapping, which confirms that the trend in the plot is not caused by the geometry of the three-block setup itself. The linear trend here indicate that the specimen failure was governed by the bulk strength of the material, instead of crack initiation and propagation caused by stress concentrations. Latter would have led to more scatter in the simulation results.

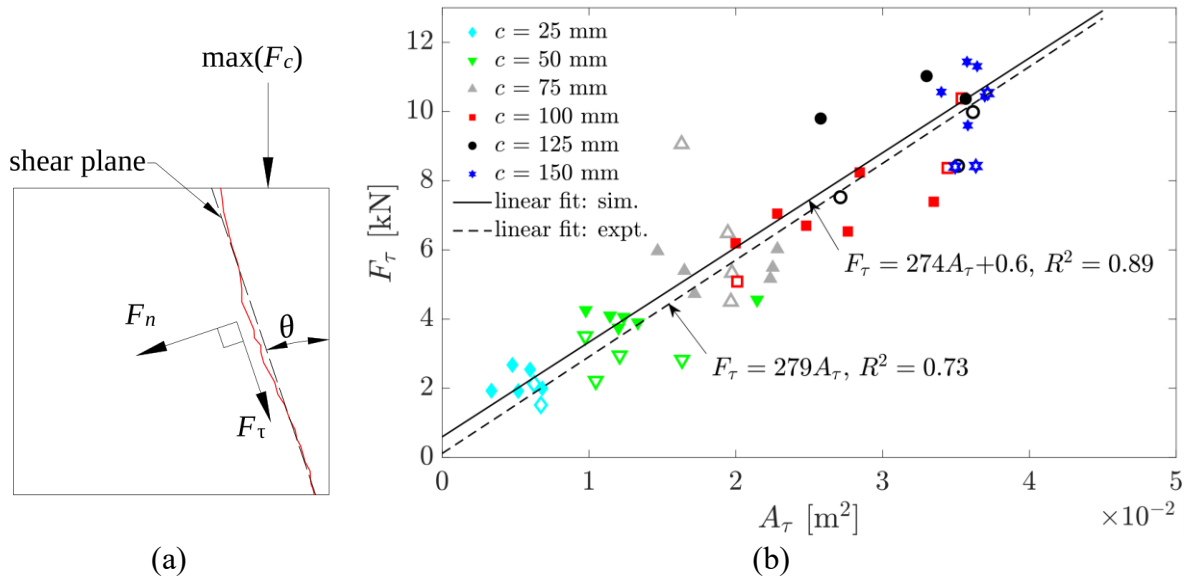

Figure 4. (a) Critical shear force, F_τ, and critical normal force, F_n, acting on a shear plane. (b) F_τ plotted against area of failure plane, A_τ. Simulation and experiment results are marked with closed and open markers, respectively. Figure reproduced from Prasanna *et al.* (2022).

The results above indicate that the ice block failure in ice-to-ice contacts can be explained using an analysis based on the strength of the materials. Therefore, it should be possible to predict the final failure planes using the pre-failure stress distribution within the ice blocks together with a strength-based failure criterion. The Mohr-Coulomb failure criterion was used here due to its simplicity and due to shear planes showing characteristics of Coulombic shear faults (Schulson *et al.*, 2006). The pre-failure stress distribution in the three-block system was obtained from the simulations by computing the Cauchy stress tensor for particles in the lattice model (Zhou, 2003). Then, the applicability of the Mohr-Coulomb failure criterion was tested by calculating the failure plane angle θ and the internal cohesion τ_0 predicted by it. Figure 5(a) presents the values of θ calculated by using the Mohr-Coulomb model and they are seem to compare well with the values of θ in the simulations and the experiments. Importantly for future modeling, the failure plane angle seem to be constant for all contact lengths. The failure planes calculated by using the Mohr-Coulomb model are presented in Figure 3 with black straight lines. They are in good agreement with the failure planes obtained from the simulations.

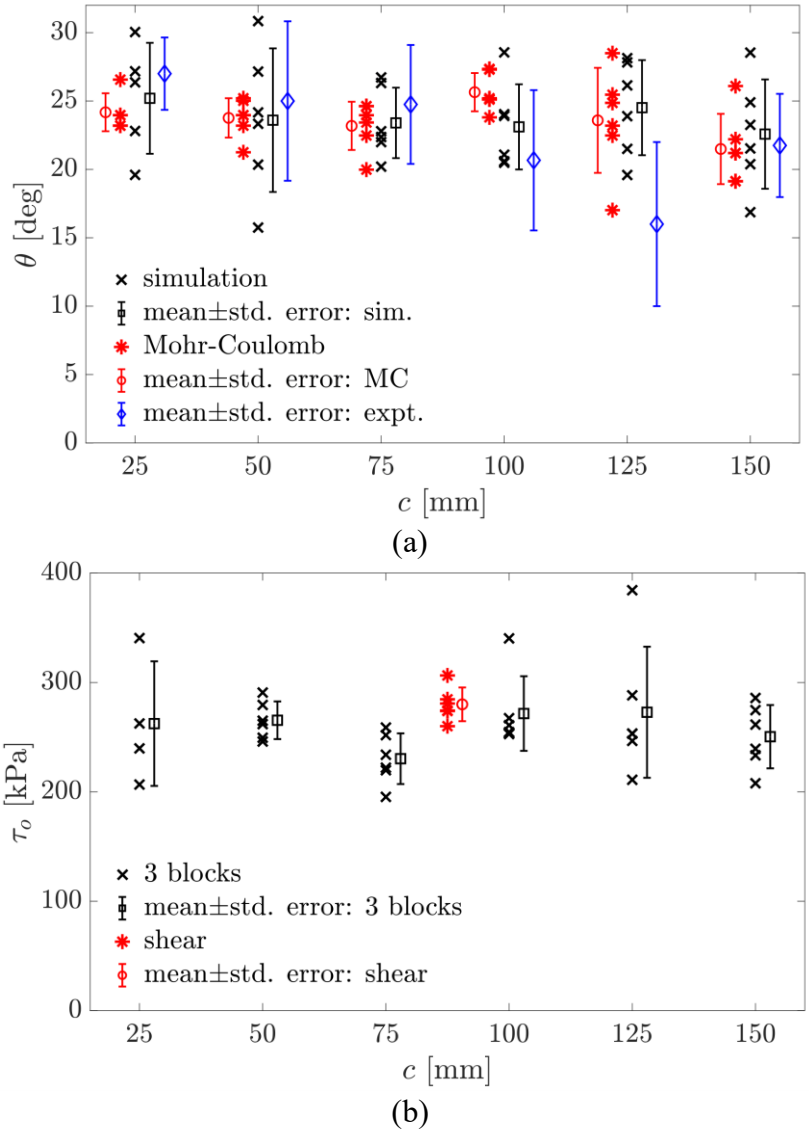

Figure 5. (a) Failure plane angles, θ, calculated using Mohr-Coulomb failure model and from the simulations. (b) Values of internal cohesion, τ_0, calculated using Mohr-Coulomb failure model. Figure reproduced from Prasanna *et al*. (2022).

Figure 5(b) shows the values for internal cohesion, τ_0, obtained from the Mohr-Coulomb failure model, plotted against the contact length, *c*. The figure also shows τ_0 calculated from simulations of an ice block failing under pure shear. The values of τ_0 from the Mohr-Coulomb model show some scatter, but their mean and the standard deviation are similar. Thus, τ_0 is approximately constant for all simulations. Moreover, the results are generally close to the values of τ_0 obtained from the pure shear simulations. This indicates that τ_0 obtained here is a property of the modeled material as it should be.

4. Discussion

Our analysis, based on the simulation data, show that the local failure of ice blocks in ice-to-ice contact occur due to shear-like failure, which can be modeled using Mohr-Coulomb failure criterion. This result stands in contrast with standard approach of using a contact force law with its upper limit based on the crushing strength of ice when modeling the contact failure of ice blocks in numerical simulations of ice-structure interaction processes (Hopkins, 1992; Paavilainen *et al*., 2009; Ranta and Polojärvi, 2019). Using a crushing strength based upper limit tends to overestimate the force transmission capacity of the contact, which could ultimately lead to overtly conservative ice load estimates on the structure (Prasanna *et al*., 2021).

Moreover, the crushing models do not predict the correct size for the ice fragments generated in the type of ice failure studied here, whereas accurate fragment size distributions might be required to capture the properties of broken ice accumulations. Therefore, a Mohr-Coulomb criterion-based shear failure model could be more suitable for modelling the local contact failure at ice-to-ice contacts. However, further effort is required to find the influence of contact geometry, loading directions related to the crystal structure and loading rate on failure mechanisms to fully understand the ice block failure in compressive ice-to-ice contacts.

The HiDEM simulation tool with the softening model developed during the work presented here was able to replicate the quasi-brittle failure of columnar grained saline ice in laboratory scale. The model could be extended to simulate full-scale ice failure by using larger ice blocks, fragments or even ice floes. However, it is not computationally realistic to use particles of millimeter scale in full-scale simulations, but, instead, particles of meter scale would be needed. The material properties of the beams would need to be recalibrated in this case. Related to this, it is important to note that HiDEM shows moderate strength weakening with increasing scales. This was tested by simulating uni-axial compressive failure of ice blocks of different sizes using the same particle size distribution and material properties for beams (Prasanna *et al*., 2022). The compressive strength of ice blocks decreased with increasing size in the simulations as it has been observed in full-scale (Weiss *et al*., 2022).

The ice tested in Prasanna *et al*. (2021) was floating in water and had an average temperature of -2.5 ºC. Therefore, HiDEM was set-up to simulate ice in relatively warm temperatures. The colder ice would have higher strength and more brittle failure characteristics. Therefore, beam properties in HiDEM must be changed if one wishes to simulate colder ice. The tensile strength and the width of the beams can be increased to replicate the increase in strength and brittleness, respectively. It is important to also note that the AMSM lattice topology developed is related to the columnar grain structure of naturally grown ice. Thus, to simulate other types of ice, lattice topology might need to be changed to replicate the relevant grain structure. For example, a random 3D lattice could work for simulating granular ice or glacial ice.

5. Conclusions

In this study, we investigated the use of BPM tool HiDEM to model the quasi-brittle failure of columnar grained, saline ice in ice-to-ice contact by simulating the three-block breakage experiments of Prasanna *et al*. (2021). The simulations were able to capture the shear failure of the ice blocks due to the formation of Coulombic shear faults as observed in the experiments. Moreover, the force records from the simulations were also in agreement with experimental results confirming that our model is capable of reproducing the essential quasi-brittle failure behaviour of ice under ice-to-ice contact compression. The details of the ice block failure were studied by using the model and the implications of the results discussed. More details can be found from Prasanna *et al*. (2021, 2022)

Acknowledgments

The authors are grateful for the financial support from the Academy of Finland through the project (309830) Ice Block Breakage: Experiments and Simulations (ICEBES). The authors wish to acknowledge CSC – IT Center for Science, Finland, for computational resources under the project (2000971) Mechanics and Fracture of Ice.

References

Åström, J.A., Riikilä, T.I., Tallinen, T., Zwinger, T., Benn, D., Moore, J.C., Timonen, J., 2013. A particle based simulation model for glacier dynamics. Cryosphere 7, 1591–1602. https://doi.org/10.5194/tc-7-1591-2013

Hopkins, M.A., 1992. Numerical Simulation of Systems of Multitudinous Polygonal Blocks. In: Technical Report 92–22. CRREL, Cold Regions Research and Engineering Laboratory, 69 pp. https://hdl.handle.net/11681/9151

Jirásek, M., Bažant, Z.P., 1995. Particle model for quasibrittle fracture and application to sea ice. Journal of Engineering Mechanics 121, 1016–1025. https://doi.org/10.1061/(ASCE)0733-9399(1995)121:9(1016)

Kuehn, G.A.A., Schulson, E.M.M., Jones, D.E.E., Zhang, J., 1993. The compressive strength of ice cubes of different sizes. Journal of Offshore Mechanics and Arctic Engineering 115, 142–148. https://doi.org/10.1115/1.2920104

Paavilainen, J., Tuhkuri, J., Polojärvi, A., 2009. 2D combined finite-discrete element method to model multi-fracture of beam structures. Engineering Computations (Swansea, Wales) 26, 578–598. https://doi.org/10.1108/02644400910975397

Prasanna, M., Polojärvi, A., Wei, M., Åström, J., 2022. Modeling ice block failure within drift ice and ice rubble. Physical Review E 105, 045001. https://doi.org/10.1103/physreve.105.045001

Prasanna, M., Wei, M., Polojärvi, Arttu., Cole, D.M., 2021. Laboratory experiments on floating saline ice block breakage in ice-to-ice contact. Cold Regions Science and Technology 189, 103315. https://doi.org/10.1016/j.coldregions.2021.103315

Ranta, J., Polojärvi, A., 2019. Limit mechanisms for ice loads on inclined structures: Local crushing. Marine Structures 67, 102633. https://doi.org/10.1016/j.marstruc.2019.102633

Schulson, E.M., Fortt, A.L., Iliescu, D., Renshaw, C.E., 2006. Failure envelope of first-year Arctic sea ice: The role of friction in compressive fracture. Journal of Geophysical Research: Oceans 111, C11S25. https://doi.org/10.1029/2005JC003235

Schulson, E.M., Gratz, E.T., 1999. The brittle compressive failure of orthotropic ice under triaxial loading. Acta Materialia 47, 745–755. https://doi.org/10.1016/S1359-6454(98)00410-8

Schulson, E.M., Nickolayev, O.Y., 1995. Failure of columnar saline ice under biaxial compression: failure envelopes and the brittle-to-ductile transition. Journal of Geophysical Research 100, 22383– 22400. https://doi.org/10.1029/95jb02513

Schulson, E.M.M., Gies, M.C.C., Lasonde, G.J.J., Nixon, W.A.A., 1989. The effect of the specimen-platen interface on internal cracking and brittle fracture of ice under compression: high-speed photography. Journal of Glaciology 35, 378–382. https://doi.org/10.1017/S0022143000009308

Todd, J., Åström, J., Benn, D.I., 2018. The Helsinki discrete element model (HiDEM). https://github.com/joeatodd/HiDEM.git

Weiss, J., Girard, L., Gimbert, F., Amitrano, D., Vandembroucq, D., 2014. (Finite) statistical size effects on compressive strength, Proceedings of the National Academy of Sciences of the United States of America, 111(17), 6231-6236. https://doi.org/10.1073/pnas.1403500111

Zhou, M., 2003. A new look at the atomic level virial stress: On continuum-molecular system equivalence. Proceedings of the Royal Society A: Mathematical, Physical and Engineering Sciences 459, 2347–2392. https://doi.org/10.1098/rspa.2003.1127